XCTK2: A Kinesin-related Protein That Promotes Mitotic Spindle Assembly in *Xenopus laevis* Egg Extracts

Claire E. Walczak, Suzie Verma, and Timothy J. Mitchison

Department of Cellular and Molecular Pharmacology, University of California at San Francisco, San Francisco, California 94143-0450

Abstract. We used a peptide antibody to a conserved sequence in the motor domain of kinesins to screen a *Xenopus* ovary cDNA expression library. Among the clones isolated were two that encoded a protein we named XCTK2 for *Xenopus* COOH-terminal kinesin 2. XCTK2 contains an NH_2-terminal globular domain, a central α-helical stalk, and a COOH-terminal motor domain. XCTK2 is similar to CTKs in other organisms and is most homologous to CHO2. Antibodies raised against XCTK2 recognize a 75-kD protein in *Xenopus* egg extracts that cosediments with microtubules. In *Xenopus* tissue culture cells, the anti-XCTK2 antibodies stain mitotic spindles as well as a subset of interphase nuclei. To probe the function of XCTK2, we have used an in vitro assay for spindle assembly in *Xenopus* egg extracts. Addition of antibodies to cytostatic factor-arrested extracts causes a 70% reduction in the percentage of bipolar spindles formed. XCTK2 is not required for maintenance of bipolar spindles, as antibody addition to preformed spindles has no effect. To further evaluate the function of XCTK2, we expressed XCTK2 in insect Sf-9 cells using the baculovirus expression system. When purified (recombinant XCTK2 is added to *Xenopus* egg extracts at a fivefold excess over endogenous levels) there is a stimulation in both the rate and extent of bipolar spindle formation. XCTK2 exists in a large complex in extracts and can be coimmunoprecipitated with two other proteins from extracts. XCTK2 likely plays an important role in the establishment and structural integrity of mitotic spindles.

Mitosis is the process by which cells faithfully segregate their genetic material. Segregation of chromosomes is carried out on the mitotic spindle, which consists of a dynamic array of microtubules. Microtubules are polar polymers that exhibit nonequilibrium polymerization dynamics termed dynamic instability. This intrinsic property of microtubules is thought to play a crucial role in the assembly of the mitotic spindle. However, the process of spindle assembly and spindle function also requires an array of additional proteins. For example the separation of spindle poles, movement of chromosomes to the equatorial plate at metaphase, spindle maintenance, and the separation of sister chromatids at anaphase all require mechanical force. Many of these processes are likely to involve the use of microtubule-based motor proteins which couple the energy of ATP hydrolysis to force production (for review see Bloom and Endow, 1995; Moore and Endow, 1995; Vernos and Karsenti, 1996). Both cytoplasmic dynein and members of the kinesin-related protein (KRP)[1] family of motors have been implicated in spindle assembly and function (for reviews see Sawin and Endow, 1993 and Barton and Goldstein, 1996; Vernos and Karsenti, 1996).

Cytoplasmic dynein, one of the first motor proteins to be implicated in spindle assembly, is localized to kinetochores and spindles during mitosis (Pfarr et al., 1990; Steuer et al., 1990). Microinjection of dynein antibodies into mammalian tissue culture cells causes a mitotic arrest with unseparated centrosomes, suggesting that dynein is required in the early stages of spindle assembly (Vaisberg et al., 1993). Dynein has also been shown to be involved in aster formation and spindle pole assembly in *Xenopus* (Verde et al., 1991; Heald et al., 1996). Interestingly, this does not appear to be the case in yeast, where dynein may be more important in spindle positioning than in spindle function (Eshel et al., 1993; Li et al., 1993), although dynein activity may also contribute to anaphase spindle elongation (Saunders et al., 1995). These results leave the universal theme of dynein function in mitosis unclear but highlight the importance of understanding dynein function in different experimental systems.

Please address all correspondence to Claire Walczak, Department of Cell and Molecular Pharmacology, University of California at San Francisco, 513 Parnassus Box 0450, San Francisco, CA 94143-0450. Tel.: (415) 476-0836; Fax.: (415) 476-5233; E-mail: walczak@cg1.ucsf.edu

1. *Abbreviations used in this paper*: CSF, cytostatic factor-arrested; CTK, carboxy-terminal kinesin; KRP, kinesin-related protein.

In addition to dynein, KRPs in the bimC and KAR3 families also function in spindle assembly. The mitotic motor field exploded following the finding that mutations in the *Aspergillus bimC* gene, which encodes a protein with homology to kinesin (Enos and Morris, 1990), exhibit defects in spindle pole body separation and mitotic spindle formation. Homologs to *bimC* have been isolated from widely divergent organisms including yeast, *Xenopus*, *Drosophila*, and humans. *Xenopus* Eg5 and *Drosophila* KLP61F have been analyzed biochemically and shown to be slow (1–3 μm/min), plus-end directed microtubule motors (Sawin et al., 1992; Cole et al., 1994; Barton et al., 1995; Kashina et al., 1996). In addition, several members of this family of KRPs have been localized to mitotic spindles (Hagan and Yanagida, 1992; Hoyt et al., 1992; Roof et al., 1992; Sawin et al., 1992; Barton et al., 1995). All bimC family members appear to be conserved in function and are involved in either spindle pole formation and/or separation. In addition to their role in spindle pole separation, a genetic analysis of bimC family members suggests that some of these motors, in combination with motors in the KAR3 family, may be important in maintaining a force that stabilizes the mitotic spindle.

The KAR3 family of kinesins may provide a force that directly opposes that of the bimC family and therefore may work to stabilize spindles. *KAR3* encodes a protein that belongs to the family of KRPs that have their motor domain at the COOH-terminal end of the protein. In *Saccharomyces cerevisiae*, deletion of *KAR3* suppresses a double knockout of the redundant bimC family genes *CIN8*/*KIP1*, suggesting an antagonistic force relationship between these two families of KRPs (Saunders and Hoyt, 1992; Roof et al., 1992; Hoyt et al., 1993). Members of the KAR3 family of KRPs, including *Drosophila* ncd and CHO2, have been localized to mitotic spindles and show minus-end directed microtubule motility in vitro (McDonald et al., 1990; Meluh and Rose, 1990; Walker et al., 1990; Hatsumi and Endow, 1992*a*; Endow et al., 1994; Kuriyama et al., 1995; Pidoux et al., 1996). Biochemical and mutant analysis of the KAR3 family of KRPs suggests that their function may involve bundling microtubules during mitotic spindle assembly (McDonald et al., 1990; Meluh and Rose, 1990; Chandra et al., 1993; Hatsumi and Endow, 1992*a*,*b*; Endow et al., 1994; Kuriyama et al., 1995; Matthies et al., 1996; Pidoux et al., 1996). Despite the large number of studies on KAR3 and other COOH-terminal family KRPs, their precise function and mechanism of action remains elusive.

To study the role of KRPs in mitosis, we isolated KRPs from *Xenopus* that might be important in spindle assembly and function (Walczak et al., 1996). One of the clones identified encodes a protein which we named XCTK2 (for *Xenopus* COOH-terminal kinesin 2). XCTK2 localizes to the mitotic spindle and is important for normal mitotic spindle assembly in vitro. Furthermore, addition of purified, recombinant XCTK2 to extracts stimulates both the rate and extent of spindle formation. Hydrodynamic analysis showed that XCTK2 is present in a large protein complex in extracts, and that the motor is the limiting component of this complex. These results suggest that XCTK2 is important for spindle formation, and the level of this protein may be crucial in controlling the kinetics of spindle formation in vivo.

Materials and Methods

Isolation of XCTK2 Clone

Affinity purified anti-HIPYR peptide antibody (Sawin et al., 1992*b*) was used to screen a λUni-ZAP *Xenopus* ovary cDNA library (Strategene, La Jolla, CA) as described previously (Walczak et al., 1996). We found that 2/75 clones encoded XCTK2. A single cDNA clone, clone 24G, was fully sequenced on both strands using Sequenase Version 2.0 (United States Biochem. Corp., Cleveland, OH). Gaps and ambiguities were resolved by using an automated DNA sequencer (performed by the Biomolecular Resource Center DNA Sequencing Facility, the University of California at San Francisco).

Protein Expression and Antibody Production

The region corresponding to amino acids 2–289 was amplified using PCR and cloned into pRSETB (Invitrogen, San Diego, CA) to produce a 6-His fusion protein (clone pRSET24GNM) and into pGex-1 (Smith et al., 1988) to produce a GST fusion protein (clone pGex-24GNM). The 6-His fusion protein was used for rabbit antibody production (Berkeley Antibody Co., Richmond, CA), and the antibodies were affinity purified according to published procedures (Harlow and Lane, 1988) on the GST fusion protein. Antibodies (anti-XCTK2) were eluted from the affinity column with 100 mM glycine, pH 2.5, 150 mM NaCl, neutralized, and then dialyzed against 10 mM Hepes, pH 7.2, 100 mM KCl before being concentrated for use in the experiments described.

A COOH-terminal peptide antibody (anti–XCTK2-CTP) was generated against the synthetic peptide CVIGTARANRK (synthesized by the University of California at San Francisco, Biomolecular Resource Center), which corresponds to the last 11 amino acids of XCTK2. All peptide conjugation procedures and antibody affinity purification were as described (Sawin et al., 1992*b*). Antibodies (anti-CTP1) were dialyzed and concentrated as described.

MT Pelleting Assays and Immunoblotting

High speed supernatants of *Xenopus* egg extracts were prepared from crude cytostatic factor-arrested (CSF) extracts (Murray, 1991) as described previously (Hirano and Mitchison, 1993). Microtubule pelleting assays were performed as described previously (Walczak et al., 1996).

SDS-PAGE and electrophoretic transfer were according to routine protocols (Harlow and Lane, 1988). Immunoblots were blocked at least 2 h in 5% NFDM (nonfat dry milk) in TBST (20 mM Tris, pH 7.4, 150 mM NaCl, 0.1% Tween 20) with 0.1% NaN_3, rinsed, and incubated in primary antibody (0.5 μg/ml anti-XCTK2 or 5 μg/ml anti-CTP1) diluted in 2% BSA in TBST with 0.1% NaN_3, followed by horseradish peroxidase-conjugated secondary antibody (1:2,500). Blots were rinsed and developed with enhanced chemiluminescence (Amersham Intl., Buckinghamshire, UK).

Immunofluorescence

XL177 cells were grown on polylysine-coated glass coverslips to near confluency. Coverslips were rinsed in TBS, and then cells were fixed with −20°C MeOH for 5 min. Coverslips were processed essentially as described (Sawin et al., 1992*b*). All micrographs were taken on a laser scanning confocal microscope (MRC-600; BioRad Laboratories, Cambridge, MA). Series of optical sections through the cell were collected and projected onto a single image plane. Images were transferred to Adobe Photoshop, digitally processed, assembled in Microsoft PowerPoint, and printed on a Tektronix Phaser 440 printer.

Extract assembled spindles were prepared as described. After methanol fixation, coverslips were washed in TBS–TX (TBS with 0.1% Triton X-100), blocked, and stained with primary and secondary antibodies. DNA was visualized with 10 μg/ml Hoechst 33258, and the coverslips were mounted. Photomicrographs were taken on a Nikon Optiphot-2 with a 40× objective (Planfluor 0.75 NA) and a cooled CCD camera (Princeton Sci. Instr. Inc., Monmouth Junction, NJ). Images were transferred to Adobe Photoshop and processed as described.

Expression of XCTK2 in Insect Sf-9 Cells and Purification

The full length XCTK2 clone 24G was inserted into the BamHI to KpnI sites of the transfer vector pVL1393N, which is a modified version of

pVL1393 (Pharmingen, San Diego, CA) in which an NcoI linker was introduced at the SmaI site. Insect Sf-9 cells were cotransfected with the transfer vector and BaculoGold virus DNA (Pharmingen) using calcium–phosphate precipitation. Transfection supernatants were plaque purified, and baculovirus stocks were amplified and used for infections. Infected Sf-9 cells were isolated and resuspended in 1:10 volume of lysis buffer (80 mM Pipes, pH 6.8, 1 mM $MgCl_2$, 1 mM EGTA, 0.1 mM EDTA, 100 mM NaCl, 1 mM DTT, 2 mM Mg-ATP, 1 mM PMSF, 1 μg/ml LPC [leupeptin, pepstatin A, chymostatin]) and sonicated for 1 min with a tip sonicator at 4°C. The lysate was centrifuged at 12,000 rpm for 10 min in an SS-34 rotor. The resulting supernatant was filtered through a 0.2 μm syringe filter before loading on the column. The sample was run on a 1 ml HiTrap™SP column equilibrated in Pipes low salt column buffer (PCB-lo: 20 mM Pipes, pH 6.8, 1 mM $MgCl_2$, 1 mM EGTA, 0.1 mM EDTA, 100 mM NaCl, 1 mM DTT, 50 μM Mg-ATP, 0.1 μg/ml LPC) and then eluted with a linear 100–500 mM NaCl gradient in PCB. Peak XCTK2 fractions were eluted at ~300 mM NaCl, pooled and concentrated, and then run on a Superose 6 gel filtration column (Pharmacia Fine Chemicals, Piscataway, NJ) in PCB-lo. The peak fractions were pooled, sucrose was added to 10% wt/vol, and then the samples were quick frozen in liquid nitrogen and stored at −80°C.

Spindle Assembly

CSF extracts were prepared essentially as described (Murray, 1991), except that the crushing spin was performed at 10,000 rpm, for 15 min, and with full brake in an SW55 Ti rotor (Beckman Instruments, Fullerton, CA). Mitotic spindle assembly was carried out as described (Sawin and Mitchison, 1991), using freshly prepared extracts. The final concentration of sperm nuclei was 150 sperm/μl. For most experiments, we used CSF extract assembled spindles. For some antibody addition experiments and for immunofluorescent staining of spindles, CSF extracts were cycled into interphase with the addition of Ca^{2+} and then back into mitosis with fresh CSF extract as described (Sawin and Mitchison, 1991; Shamu and Murray, 1992). Results from the two different types of extract preparation were similar. For antibody addition experiments, antibodies were added as 1:10 final volume diluted in sperm dilution buffer (5 mM K-Hepes, pH 7.7, 1 mM $MgCl_2$, 100 mM KCl, 150 mM sucrose). Immunodepletion experiments were carried out as described previously (Walczak et al., 1996). For excess XCTK2 addition, protein was added as 1:10 final volume at the time of sperm addition. The amount of excess XCTK2 protein was compared to the endogenous level of XCTK2 by quantitative immunoblotting. We estimate that the total XCTK2 concentration in these samples was ~10 μg/ml compared to an endogenous concentration of 1–2 μg/ml.

For quantitation, spindles were assembled as described, and at the indicated time point, 20 μl of the extract was removed and diluted into 2 ml of BRB80, 30% glycerol, 0.5% TX-100, 1 mM Mg-ATP. This was layered onto a cushion containing BRB80, 40% glycerol, 1 mM Mg-ATP and centrifuged onto coverslips at 6,000 *g* for 30 min. Coverslips were postfixed in −20°C methanol, washed in TBS–TX, and processed as described for immunofluorescence. The results presented represent quantitated data from four individual experiments in three separate extracts with at least 200 nuclei counted per time point. We qualitatively observed the same results with at least five independent extracts.

Hydrodynamic Analysis and Immunoprecipitations

All of the hydrodynamic analyses were carried out on either *Xenopus* egg high speed supernatants, 25% ammonium sulfate supernatants, or Sf-9 cell supernatants. The stokes radius of XCTK2 was estimated by gel filtration on a Superose 6 column (Pharmacia Fine Chemicals) calibrated with the standards thyroglobulin (8.5 nm), ferritin (6.1 nm), aldolase (4.81 nm), and ovalbumin (3.05 nm). Sedimentation coefficients ($S_{20,w}$) were determined by centrifugation on 5–20% sucrose gradients in an SW55 or a TLS-55 rotor for 12 h at 4°C at 40,000 rpm in PCB with either 100 mM NaCl (PCB-lo) or 1 M NaCl (PCB-hi). The gradients were calibrated on each run with catalase (11.3S), bovine serum albumin (4.4S), and ovalbumin (3.6S). The molecular weight of the protein was estimated by the method of Siegel and Monty (1966).

The position of XCTK2 on the column or gradients was determined by ELISA. Either 25 or 50 μl of each fraction was coated into polyvinyl chloride plates for 1 h at room temperature. Excess antigen was removed, and the wells were blocked for 1 h at room temperature in 5% NFDM in TBST. The blocking solution was removed and the wells were rinsed four times with TBST. Primary antibody (2 μg/ml anti-XCTK2) was incubated for 1 h at room temperature. The plates were washed four times with TBST and then incubated with 1:5,000 alkaline phosphatase-conjugated secondary antibody. The plates were washed four times and developed with 1 mg/ml p-nitrophenyl phosphate in 50 mM $NaHCO_3$, pH 10, 0.5 mM $MgCl_2$. Absorbance at 410 nm was read on a Dynatech ELISA reader.

For immunoprecipitations, affi-prep protein A beads were washed three times in TBS–TX and then coated with affinity purified anti-XCTK2 antibodies, anti-CTP1 antibodies, or control IgG for 1 h. We used a ratio of 2 μg antibody/12.5 μl beads/100 μl extract. After antibody binding, the beads were washed one time in TBS–TX and four times in CSF–XB (10 mM K-Hepes, pH 7.7, 50 mM sucrose, 2 mM $MgCl_2$, 0.1 mM $CaCl_2$, 100 mM KCl, 5 mM EGTA, 1 μg/ml LPC). The washed beads were added to egg high speed supernatants supplemented with recombinant XCTK2 to bring the final XCTK2 concentration to ~10 μg/ml and incubated for 1 h at 4°C. The high speed supernatants had been diluted 1:1 with CSF–XB and then clarified for 10 min in a microfuge before addition to the beads. The beads were washed two times with CSF–XB, four times with TBS–TX, and then boiled in sample buffer before running on a gel. Under conditions where recombinant XCTK2 was not added to the extract during immunoprecipitation, it was difficult to distinguish which bands were coprecipitating specifically due to the low abundance of this protein.

Results

Identification and Characterization of XCTK2

To find KRPs involved in mitotic spindle assembly and function, we screened a *Xenopus* ovary cDNA library with the anti-HIPYR peptide antibody as described previously (Walczak et al., 1996). Among the clones isolated were two cDNAs that encoded XCTK2. The cDNA for XCTK2 is 2,837 nucleotides in length and encodes a 643–amino acid protein with a predicted molecular mass of 72 kD (Fig. 1). Structural predictions based on the amino acid sequence suggest that the XCTK2 protein consists of a 120–amino acid NH_2-terminal globular domain, a central 170–amino acid α-helical coiled-coil domain, and a COOH-terminal kinesin-like motor domain. In a phylogenetic analysis, XCTK2 groups with a family of KRPs with COOH-terminal motor domains that include ncd and KAR3 (see Moore and Endow, 1995, for a phylogenetic tree). XCTK2 is most closely related to the mammalian CH02 protein (Kuriyama et al., 1995) and human HSET (Ando et al., 1994).

To study the function of XCTK2 in *Xenopus* we raised polyclonal antibodies (*anti-XCTK2*) to the NH_2-terminal 289 amino acids of XCTK2 which include the globular domain and the coiled coil domain (Fig. 2 *A*). We also made an anti-peptide antibody to the last 11 amino acids of the protein (*anti-CTP1*). Both of these antibodies recognize a

```
MDSTDKKVQV ASRLPVPPKR KYVSNDENQE QMQRKRLRSS LESELPAVRV    50
AASIATSKPR AAPVAALPKP QVIGRQSLAV MRPKNSGPGI TSTSFSGKTK   100
VSSSVTQPAA IGAEKKKRAA WDLKGQVNDM RDTVSNYKGK MQNLTGENAR   150
LLNSKEKLQR EVEVLASENS KLSQERCTLE SQLREVRQQV STFEREVARL   200
TELCQRQEKE LSSHTNTIEE LQGANAILTK QLLDKEVKLD CVSGENTSLK   250
HTVNEQTDEI AALKVCLAEK DTEVHSLDTE RRRLHNLVQE LKGNIRVFCR   300
VRPTLTPERE LPAGHISFPS NDGKAIVLSK MEESHIGREK KDAVKYDFNF   350
DCVFPPPCSQ ESVFEEISLL VQSALDGYPV CIFAYGQTGS GKTYTMEGPE   400
DVTDDSMGMI PRAIHQIFSS AEELKAKGWQ YTFTASFLEI YNETIRDLLI   450
NRPDKKLEYE IRKVNSANML LYVTNLRYVK VSCVEEVHEL LKIAKANRSV   500
AKTAINDRSS RSHSVFQLKI EGENKQRDLK TSSMISLIDL AGSERLDRSL   550
STGDRLKETQ CINTSLSTLG MVITSLCNKD SHIPYRNSKL TYLLQNSLGG   600
NAKVLMFVNI SPLEENFAES LNSLRFASKV NECVIGTARA NRK           643
```

Figure 1. The deduced amino acid sequence of XCTK2 indicates that it is a kinesin-related protein. The putative P-loop (nucleotide binding consensus sequence) is indicated in bold, and the conserved peptide sequence recognized by the HIPYR peptide antibody used to isolate the clone is underlined. These sequence data are available from GenBank/EMBL/DDBJ under accession number U82809.

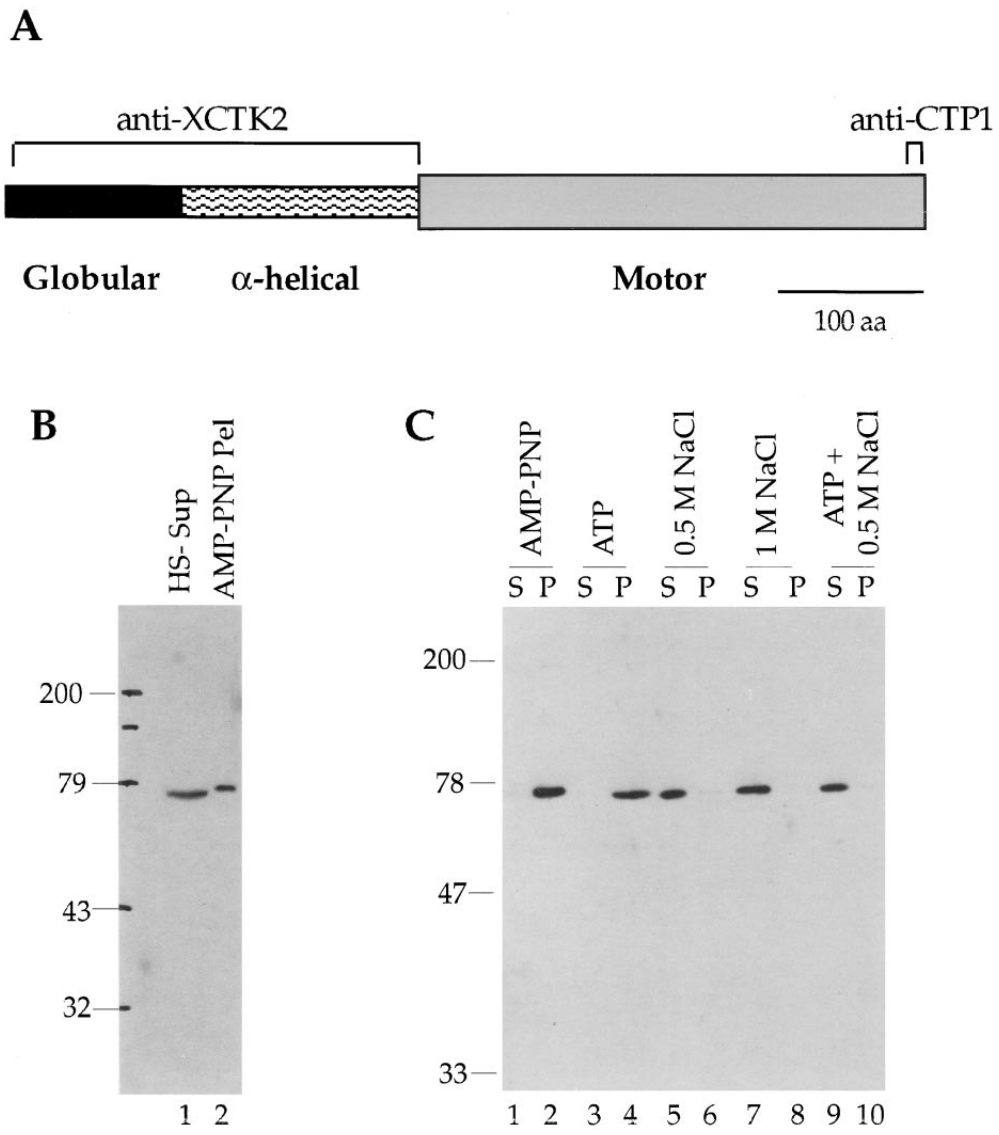

Figure 2. XCTK2 contains a COOH-terminal motor domain and binds microtubules. (*A*) A schematic representation of the predicted structure of XCTK2. XCTK2 contains an NH_2-terminal globular domain, a central α-helical stalk and a COOH-terminal motor domain. (*B* and *C*) Immunoblots of microtubule pelleting assays in *Xenopus* egg extracts. (*B*) *Xenopus* egg high speed supernatants (lane *1*) or AMP-PNP microtubule pellets (lane *2*) were probed with anti-CTP1 antibody. The slight band shift is due to the high amounts of protein present in the high speed supernatant that alter the migration of XCTK2. (*C*) Microtubules were polymerized in mitotic high speed supernatants of *Xenopus* egg extracts and pelleted in the absence of ATP and the presence of AMP-PNP (lanes *1* and *2*). The microtubule pellet, with associated proteins, was resuspended and extracted with various nucleotides and salt to generate supernatants (*S*) and pellets (*P*) of each extraction condition: 2 mM Mg–ATP (lanes *3* and *4*); 0.5 M NaCl (lanes *5* and *6*); 1 M NaCl (lanes *7* and *8*), or 2 mM Mg–ATP with 0.5 M NaCl (lanes *9* and *10*). The blots were probed with anti-XCTK2 antibody.

protein of 75 kD in *Xenopus* egg extracts, close to the predicted size of XCTK2 (Fig. 2, *B* and *C*, lanes *1* and *2*).

To show that XCTK2 had properties consistent with being a KRP, we performed microtubule binding experiments (Fig. 2, *B* and *C*). *Xenopus* egg high speed supernatants were treated with taxol, AMP–PNP, and an ATP-depletion system to polymerize microtubules. The microtubules and associated proteins were sedimented and then extracted with various combinations of nucleotide and salt. XCTK2 cosedimented with microtubules (Fig. 2, *B* and *C*, lanes *1* and *2*) under conditions of ATP depletion. XCTK2 could be released from microtubules by salt alone or by ATP and salt (Fig. 2 *C*, lanes *5–10*), but not by ATP alone.

XCTK2 Localizes to the Mitotic Spindle

We used the anti-XCTK2 antibodies to determine the localization of XCTK2 in the *Xenopus* tissue culture cell line, XL177 (Fig. 3). During interphase, anti-XCTK2 antibodies stained some nuclei and not others; the intensity of the nuclear staining varied from cell to cell and may correlate with the cell cycle state of the nuclei (Fig. 3, *I*). As the cell entered mitosis, XCTK2 was localized to the mitotic spindle during prophase, and this localization persisted through anaphase (Fig. 3, *P–A*). XCTK2 was enriched toward the spindle poles as compared to microtubules. The localization to the mitotic spindle was dependent upon the presence of microtubules as treatment of the cells with nocodazole abolished all spindle staining. At the end of mitosis, XCTK2 protein was redistributed from the spindle to the reforming daughter nuclei (Fig. 3, *T*). Sometime after cytokinesis the protein was degraded, as evidenced by the lack of staining in nuclei that had recently divided. The observed localization was competed by inclusion of the XCTK2 stalk–tail fusion protein in the primary antibody solution and was not observed with a nonimmune IgG antibody or with antibodies to several other *Xenopus* KRPs, indicating that the staining is specific for XCTK2 antibodies (data not shown).

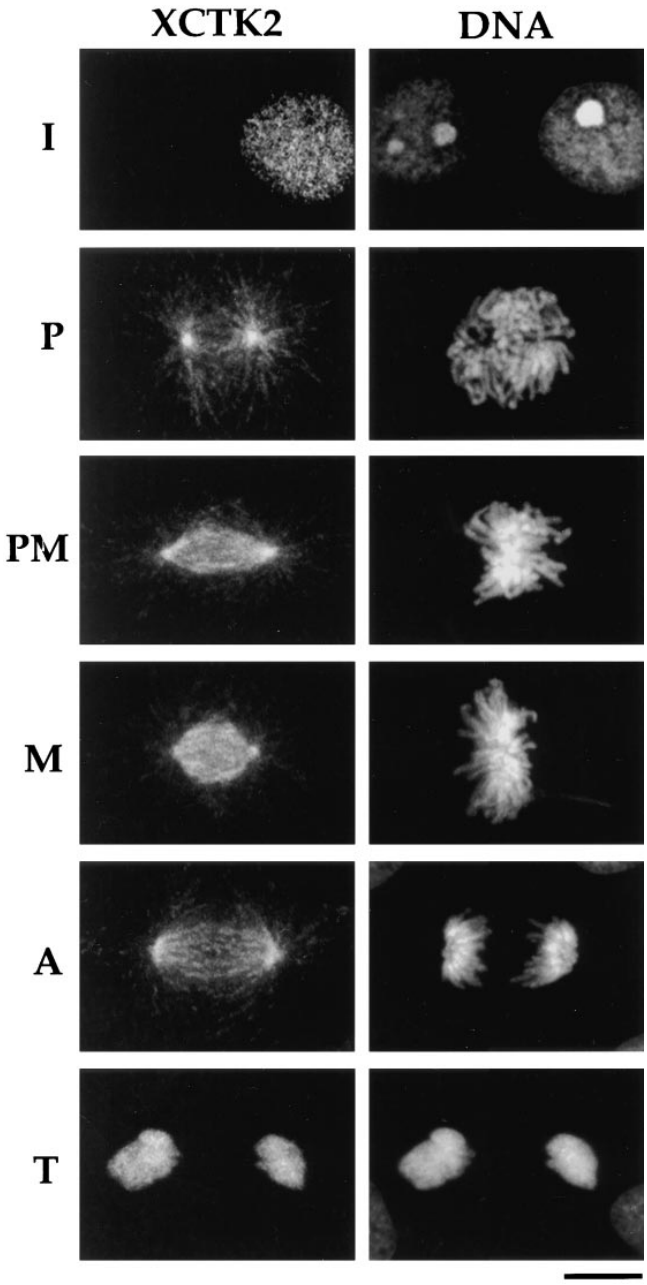

Figure 3. Immunolocalization of XCTK2 in *Xenopus* tissue culture cells. The cells were stained with 1 μg/ml anti-XCTK2 followed by FITC-conjugated goat anti–rabbit secondary antibody. DNA was visualized by staining with 0.05 μg/ml propidium iodide. Images were recorded on a laser scanning confocal microscope. Interphase (*I*); prophase (*P*); prometaphase (*PM*); metaphase (*M*); anaphase (*A*); telophase (*T*). Bar, 20 μm.

XCTK2 Is Important for Bipolar Mitotic Spindle Assembly

To probe the function of XCTK2, we examined its role in mitotic spindle assembly using *Xenopus* egg extracts. When a sperm nucleus is added to a mitotically arrested egg extract, the nucleus directs the formation of a bipolar mitotic spindle (Lohka and Maller, 1985; Sawin and Mitchison, 1991; Shamu and Murray, 1992). Two types of spindle assembly pathways have been described. In the first type of assembly, called CSF assembly, a sperm nucleus is put into a mitotically arrested *Xenopus* egg extract. A radial aster of microtubules forms around the centrosome and rearranges into a directed aster and then into a structure termed a "half spindle." Two of these half spindles then fuse to form a normal bipolar spindle. In the second type of spindle assembly reaction, called "interphase to mitosis" assembly or more commonly "cycled spindle assembly," the sperm nucleus is put into a mitotically arrested *Xenopus* egg extract which is immediately cycled into interphase by the addition of Ca^{2+}, allowing for DNA replication. The extract is then cycled back into mitosis by the addition of fresh mitotic extract. In this type of extract, a bipolar spindle forms from a single sperm nucleus in a pathway that is independent of half-spindle intermediates (Sawin and Mitchison, 1991; Shamu and Murray, 1992; Boleti et al., 1996). The cycled spindle assembly pathway represents the physiological pathway for assembly; however, the CSF assembly reaction has discrete intermediates enabling interpretation of function. Comparison of results of inhibition of protein function in both types of spindle assembly reactions should facilitate elucidating the function of that protein.

We first looked at the effect of loss of XCTK2 function on CSF spindle assembly. Either the anti-CTP1 antibody or the anti-XCTK2 antibody was added to the extract at the time of sperm addition. Spindle assembly was allowed to progress for 60 min, and then the spindles and spindle-like structures were sedimented through glycerol cushions onto coverslips. Control extracts formed a high percentage of bipolar mitotic spindles (Fig. 4 *A*). However, when XCTK2 function was inhibited, there was a 70% reduction in the percentage of bipolar spindles that formed (Fig. 4, *B–D*). Most of the structures that formed in the absence of XCTK2 function were early spindle intermediates, either asters or half spindles (Fig. 4, *B* and *C*). In some cases we noticed that the microtubules of the bipolar spindles that did form were less dense or bent and that the half spindles were often splayed, suggesting that XCTK2 is required for providing structural integrity to the spindles and intermediates. At earlier time points there was a less dramatic effect of antibody addition, suggesting that XCTK2 function is not required for aster formation or half spindle assembly but rather for the fusion of half spindles into bipolar spindles. When XCTK2 was immunodepleted from extracts before spindle assembly, a similar inhibition of bipolar spindle assembly was seen (31.5 ± 3.2% of control IgG addition; $n = 6$ experiments, 1,817 nuclei counted). However the effect appeared less dramatic, mainly because control immunodepletions cause a diminution in the fraction of bipolar spindles that form (40 ± 9.2% of control IgG addition; $n = 2$ experiments, 613 nuclei counted).

We next looked at the effect of antibody addition on the formation of cycled spindles. In the presence of either of the XCTK2 antibodies, there was a 34% reduction in the percentage of bipolar spindles that formed ($n = 8$ experiments, 1,615 nuclei counted). Again the microtubules of the spindles were sometimes less dense or bent, and a higher proportion of structures that formed were unipolar asters. This shows that even in spindles formed in the absence of half spindle fusion, there is a defect in bipolar mitotic spindle assembly, suggesting that XCTK2 is indeed

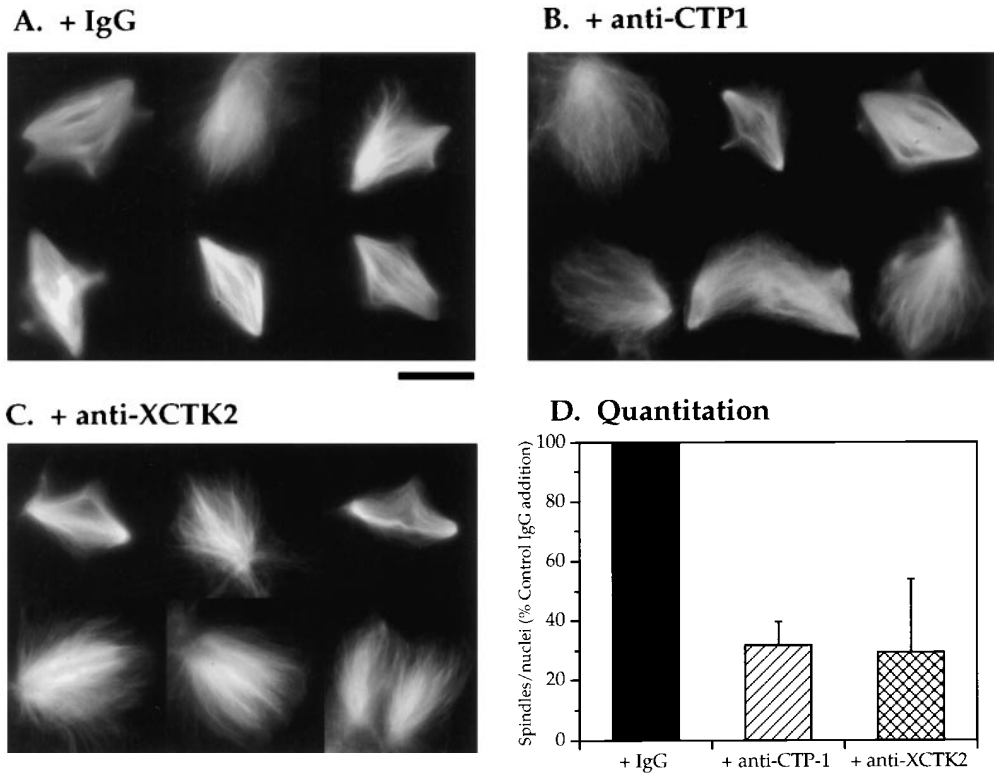

Figure 4. XCTK2 is important for mitotic spindle assembly. Mitotic spindles were assembled in the presence of either (*A*) 95 μg/ml control IgG, (*B*) 95 μg/ml anti-CTP1, or (*C*) 95 μg/ml anti-XCTK2. Spindles were assembled in CSF extracts that contained rhodamine-labeled tubulin and antibody for 60 min and then sedimented onto coverslips. In the presence of antibodies that inhibit XCTK2 function, there is a decrease in the percentage of bipolar spindles that formed. Six random structures were photographed from five fields of view, and they were compiled into the field of view that is shown. To compare between panels, count the number of bipolar spindles versus half spindles in each panel. Rhodamine-labeled microtubules are shown. Bar, 20 μm. (*D*) Quantitation of XCTK2 immunoinhibition. The percentage of half spindles, bipolar spindles, and aster-like structures that formed per nuclei were quantitated. The data are represented as the percentage of bipolar spindles that formed, normalized to the IgG control addition as 100%. The bars represent mean ± 1 SD (n = 1,020 nuclei for IgG addition [four experiments]; n = 965 nuclei for anti-CTP1 addition [four experiments]; n = 1,007 nuclei for anti-XCTK2 addition [four experiments]).

important for spindle assembly. If antibodies to XCTK2 were added to preformed spindles, there was no perturbation to the spindle structure, suggesting that XCTK2 is not required for maintenance of spindle structure.

To better understand how the XCTK2 antibodies were perturbing spindle structure, we determined the localization of the added antibodies to see if antibody addition caused mislocalization of XCTK2 during mitotic spindle assembly, which could account for the observed defects. In control spindles formed in the presence of IgG, XCTK2 protein is normally localized on mitotic spindles with an enrichment toward the poles (Fig. 5, *top panels*), similar to the localization we observed in tissue culture cells (compare with Fig. 3). In contrast, when anti-XCTK2 antibodies

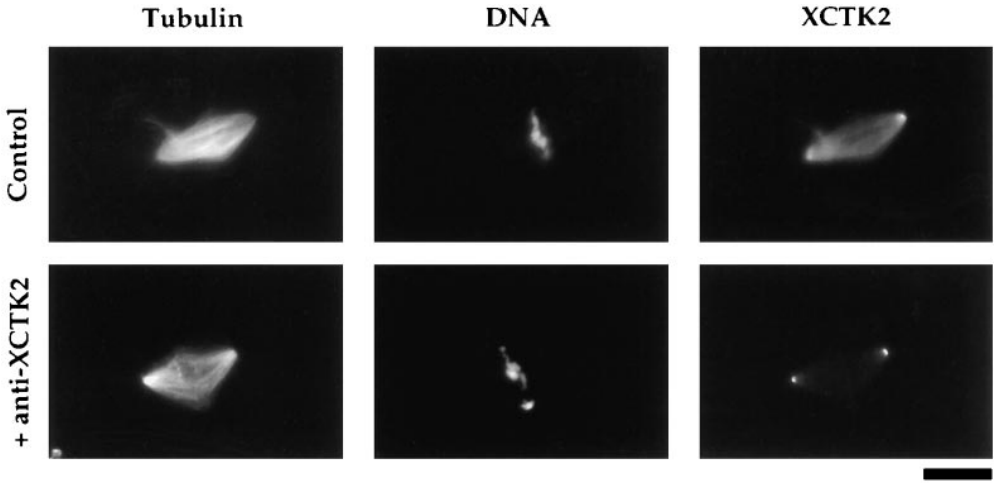

Figure 5. Anti-XCTK2 antibodies cause relocalization of XCTK2. Mitotic spindles were assembled in the presence of rhodamine-labeled tubulin in cycled CSF extracts for 60 min and then sedimented onto coverslips. (*Top*) Spindles were assembled, sedimented, fixed, and then stained with anti-XCTK2 antibodies, followed by FITC-conjugated goat anti–rabbit secondary antibody. DNA was visualized by staining with Hoechst 33528. XCTK2 stains the spindle with an enrichment toward spindle poles. (*Bottom*) Spindles were assembled in the presence of anti-XCTK2 antibody, sedimented, fixed, and then stained with FITC-conjugated goat anti–rabbit secondary antibody. DNA was visualized by staining with Hoechst 33528. XCTK2 is now concentrated at spindle poles after assembly in the presence of anti-XCTK2 antibodies. Bar, 20 μm.

were added to extracts before spindle assembly, the XCTK2 protein became mislocalized and was highly enriched at spindle poles (Fig. 5, *bottom panels*). The shift in localization toward the poles and the resulting absence of XCTK2 in the main part of the spindle may account for the splayed structures often observed in the antibody treated extracts. The anti-XCTK2 antibody was raised against the stalk–tail region of XCTK2, which in other COOH-terminal kinesins has been shown to contain an additional ATP-independent microtubule binding domain (Chandra et al., 1993; Kuriyama et al., 1995). By binding to the stalk–tail region of XCTK2, these antibodies may inhibit binding of this domain of XCTK2 to microtubules. This inhibition of binding would free the motor domain to walk toward the minus end of microtubules and accumulate at the spindle pole. We interpret this data as evidence that XCTK2 is a minus end directed motor like other COOH-terminal kinesins. In support of this idea, if a similar experiment is done with anti-Eg5 stalk–tail antibodies, the plus end directed Eg5 motor accumulates at the plus ends of the microtubules near the chromatin (Walczak, C.E., and T.J. Mitchison, unpublished observation). Interestingly, when antibodies are added to preformed spindles, XCTK2 protein also becomes mislocalized, which suggests that correct localization of XCTK2 is important for spindle formation but not for maintenance of spindle structure.

Overaddition of XCTK2 to Extracts Stimulates Spindle Formation

To further study the role of XCTK2 in mitotic spindle assembly, we expressed full length XCTK2 in insect Sf-9 cells using the baculovirus expression system. XCTK2 was expressed at high levels and was purified by a combination of ion exchange and gel filtration chromatography (Fig. 6). In the first step of the purification, XCTK2 was bound to SP-Sepharose and eluted with 300 mM NaCl. The pooled fraction from the SP-Sepharose was then run on a Superose-6 gel filtration column. XCTK2 eluted as a broad peak with a Stokes radius of ~7.2 nm. The peak fractions were pooled and frozen in aliquots for use in the experiments below. We estimate that XCTK2 is ~90% pure by this technique (Fig. 6).

We tried many conditions to determine the velocity and directionality of XCTK2-directed motility, but we were unsuccessful. The purified protein strongly bundled microtubules and bound these microtubule bundles to the coverslip surface; however upon ATP addition there was no movement. If we first bound the anti-XCTK2 antibodies to the coverslip and then the purified XCTK2 protein, there was an inhibition of microtubule bundling at the coverslip surface but still no movement. The inhibition of microtubule bundling by anti-XCTK2 antibodies supports our interpretation of XCTK2 mislocalization during spindle assembly (see discussion of Fig. 5).

XCTK2 is present at 1–2 μg/ml in *Xenopus* egg extracts (determined from quantitative immunoblots). This is ~5–10-fold lower than the concentration of other KRPs in extracts (Vernos et al., 1995; Walczak et al., 1996; Walczak, C.E., and T.J. Mitchison, unpublished observations). We wanted to test what would happen if we increased the level of XCTK2, essentially mimicking a genetic overexpression

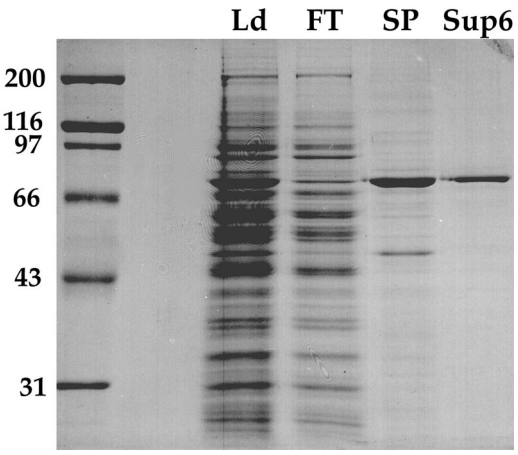

Figure 6. Purification of XCTK2. XCTK2 was expressed in insect Sf-9 cells using the baculovirus expression system. Lysates were made of infected Sf-9 cells, centrifuged and filtered through an HPLC syringe filter, run on a SP-Sepharose column (Hi-Trap™; Pharmacia Fine Chemicals) and eluted with a linear 100–500 mM NaCl gradient. The peak fractions were pooled, concentrated, and run on a Superose 6 gel filtration column. The peak fractions were pooled, sucrose was added to 10% final wt/vol, and they were frozen in 15 μl aliquots at −80°C until use in the experiments described. Fractions from the purification were run on 10% SDS-PAGE and visualized by staining with Coomassie. (*Ld*) SP-Sepharose column load. (*FT*) SP-Sepharose column flow-through. (*SP*) Pool of peak XCTK2 containing fractions from SP-Sepharose column. (*Sup6*) Pool of peak XCTK2 containing fractions from Superose 6 column. Molecular mass markers are shown on the left side of the gel.

experiment. Baculovirus-expressed and purified XCTK2 was added to CSF extracts before spindle assembly. We then monitored spindle assembly at various time points and quantitated the percentage of spindles and spindle intermediates that formed over time. Addition of a three- to fivefold excess of XCTK2 over endogenous levels increased the rate and extent of bipolar spindle formation in extracts (Fig. 7). At early time points ($t = 15'$), extracts treated with either a mock buffer control or a heat-inactivated XCTK2 control formed mostly asters or directed asters, which are structures in which the microtubules have begun to concentrate toward the DNA but have not yet organized into half spindles. In contrast, >60% of the structures containing excess XCTK2 had already formed half spindles (Fig. 7 *D*). The most striking time point was at $t = 30$ min. In the controls, the majority of the structures observed were half spindles (Fig. 7, *A*, *C*, and *E*), whereas in the presence of excess XCTK2, nearly 90% of the structures were bipolar spindles (Fig. 7, *B* and *E*). By 60 min, only ~40% of the control samples had formed bipolar spindles, yet nearly 90% of the samples containing excess XCTK2 formed bipolar spindles (Fig. 7 *F*). The spindles that formed in the presence of excess XCTK2 often contained tightly bundled microtubules, supporting our observation that XCTK2 has a bundling activity. Indeed, the purified recombinant XCTK2 was able to bundle microtubules in vitro (data not shown). These results taken together with the results from immunoinhibition experiments suggest that XCTK2 may be important in regulating the extent and timing of bipolar mitotic spindle formation.

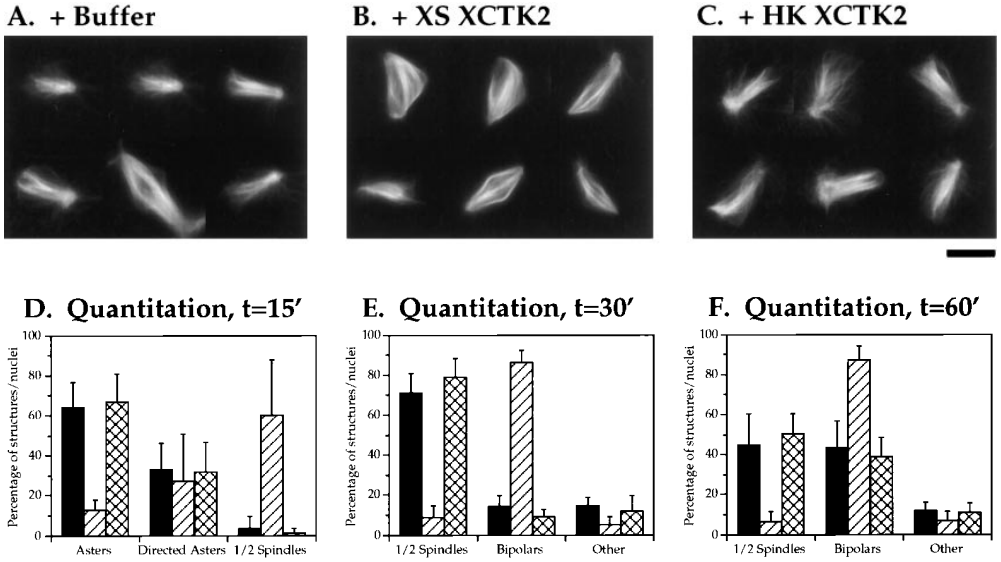

Figure 7. Addition of excess XCTK2 stimulates mitotic spindle assembly. Mitotic spindles were assembled in the presence of either (*A*) control buffer, (*B*) ~10 μg/ml XCTK2, or (*C*) ~10 μg/ml XCTK2 that had been heat killed for 5 min at 70°C before use. Spindles were assembled in CSF extracts that contained rhodamine-labeled tubulin and buffer or XCTK2 protein for 30 min and then sedimented onto coverslips. In the presence of excess XCTK2 protein, there is an increase in the percentage of bipolar spindles that formed. Six random structures were photographed from four to six fields of view, and they were compiled into the field of view that is shown. Rhodamine-labeled microtubules are shown. (*D–F*) Quantitation of excess XCTK2 addition. Spindles were assembled in CSF extracts in the presence of control buffer (*black bar*), ~10 μg/ml XCTK2 (*hatched bar*), or ~10 μg/ml heat-killed XCTK2 (*cross-hatched bar*) for 15–60 min and then sedimented onto coverslips. The percentage of asters, directed asters, and half spindles were quantitated at the 15 min time point, and the percentage of half spindles, bipolar spindles, and other structures that formed per nuclei were quantitated at the 30 and 60 min time points. The data are represented as mean ± 1 SD of four independent experiments ($n \geq 800$ nuclei for IgG addition; $n \geq 800$ nuclei for anti-CTP1 addition; $n \geq 800$ nuclei for anti-XCTK2 addition for each time point). Bar, 20 μm.

XCTK2 Exists in a Complex with Other Proteins in Extracts

To begin to examine how XCTK2 functions in spindle assembly at a molecular level, we analyzed the hydrodynamic properties of XCTK2 in extracts under conditions of low and high salt (Table I). Under low salt conditions, XCTK2 has an S value of 13S and a Stokes radius of 8.8 nm which yields a predicted molecular mass of nearly 500 kD, suggesting that XCTK2 exists in a large complex. In 1 M NaCl, XCTK2 has an S value of 5.9S and a Stokes radius of 8.0 nm which yields a predicted molecular mass of 200 kD, suggesting that this complex can be partially disrupted by high salt. Using either crude or partially purified extracts from insect Sf-9 cells expressing recombinant XCTK2, we estimated an S value of 5.1S and a Stokes radius of 7.3 nm, yielding a predicted molecular mass of 158 kD, which is consistent with that of a simple dimer.

We next analyzed whether the recombinant XCTK2 that was added to the extracts was present as a simple dimer or whether it was present in the larger complex that contained the endogenous XCTK2. All of the excess recombinant XCTK2 that was added to the extract was present in the larger 13S complex containing the endogenous XCTK2, indicating that the recombinant XCTK2 became associated with other proteins after addition to the extract. These results suggest that XCTK2 is the limiting component of this protein complex. To analyze the composition of the large complex that contains XCTK2, the XCTK2 was immunoprecipitated from *Xenopus* egg extract high speed supernatants (Fig. 8). XCTK2 and several coprecipitating proteins could be immunoprecipitated from extracts using either the anti-CTP1 peptide antibodies or the anti-XCTK2 stalk–tail antibodies (data not shown). Because of the low levels of endogenous XCTK2, it was difficult to cleanly immunoprecipitate sufficient quantities of protein to determine which coprecipitating bands were specific and which were due to background. To help overcome this problem, we supplemented extracts with recombinant XCTK2 to the same level, which caused increased spindle assembly (Fig. 7). The immunoprecipitations from the extracts that contained recombinant XCTK2 clearly showed that XCTK2 coprecipitated with one or two other

Table I. Hydrodynamic Properties of XCTK2

Sample	S value	Stokes radius	Estimated mol wt
Extract-lo salt	13 ± 1.5	8.8 ± 0.6 nm	487,000
Extract-hi salt	5.9 ± 1.2	8.0 ± 0.2 nm	202,000
BV expressed	~5.1	~7.3 nm	~158,000

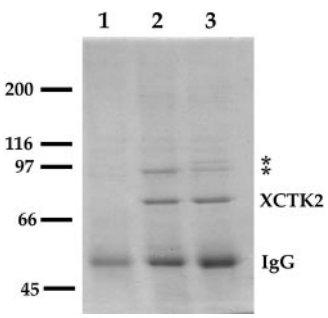

Figure 8. Immunoprecipitation of XCTK2 from egg extracts. Immunoprecipitation was performed using control rabbit IgG (lane *1*), affinity-purified anti-CTP1 (lane *2*), or affinity-purified anti-XCTK2 (lane *3*). Antibody was bound to protein A beads and then incubated in *Xenopus* egg high speed supernatants that contained ~10 μg/ml XCTK2. The protein A complexes were washed, separated by 7.5% SDS-PAGE, and visualized by staining with Coomassie.

proteins, depending on the antibody used, whose levels were significantly above the level of control immunoprecipitations (Fig. 8, lanes *1–3*). The same bands were visible in immunoprecipitations without addition of excess XCTK2, although other presumably nonspecific bands tended to obscure them.

Discussion

The COOH-terminal Family of KRPs

XCTK2 belongs to the family of KRPs, which in contrast to kinesin and most other KRPs, have their motor domain at the COOH terminus of the protein and move toward the minus end of microtubules (for reviews see Moore and Endow, 1995 and Barton and Goldstein, 1996). COOH-terminal KRPs may be important in mitotic spindle formation and stability. The best studied member of this family is *Drosophila ncd* which was isolated as a mutant that had high levels of chromosome loss and nondisjunction in *Drosophila* meiosis and early mitosis (Davis, 1969). Subsequent studies have shown that *ncd* mutants form abnormal meiotic and mitotic spindles that contain multiple or splayed poles as well as abnormal chromosome configurations (Hatsumi and Endow, 1992*b*). These studies support a model in which ncd acts to bundle microtubules and draw the minus ends of microtubules into a focused spindle pole (for reviews see Moore and Endow, 1995 and Barton and Goldstein, 1996).

Yeast *KAR3* is the next most extensively characterized COOH-terminal kinesin. *KAR3* mutants display a defect in karyogamy and subtle defects in mitosis (Meluh and Rose, 1990). KAR3 is thought to act in karyogamy by cross-linking antiparallel microtubules and drawing the two nuclei together by walking toward the minus ends of microtubules. In mitosis, KAR3 is thought to act by providing a counter balancing force to CIN8/KIP1 that acts to maintain the intact spindle (Saunders and Hoyt, 1992). Similar counterbalancing forces have been reported in *Aspergillus* and *Schizosaccharomyces pombe* (O'Connell et al., 1993; Pidoux et al., 1996). These studies support the second widely accepted model for COOH-terminal kinesin function in that this motor is important for maintaining spindle stability by counterbalancing the forces produced by the bimC family of KRPs (for reviews see Moore and Endow, 1995 and Barton and Goldstein, 1996).

XCTK2 Functions in Mitotic Spindle Assembly

Our results demonstrate that XCTK2 is important for spindle formation in vitro in *Xenopus* egg extracts. XCTK2 is localized to mitotic spindles with an enrichment toward spindle poles both in tissue culture cells and in spindles assembled in vitro. Although we have not yet been able to demonstrate in vitro microtubule motility on our preparations of XCTK2, we expect that it is a minus end directed motor by analogy to other members of the COOH-terminal family of KRPs (McDonald et al., 1990; Walker et al., 1990; Endow et al., 1994; Kuriyama et al., 1995). In addition, the observation that antibodies to the nonmotor region of XCTK2 cause the protein to relocalize to the spindle poles supports the notion that XCTK2 is a minus end directed microtubule motor.

As discussed above, we would expect that XCTK2 is required for either spindle pole formation or for providing an inward directed force required for spindle stability. Our results do not support the idea that XCTK2 is required for spindle pole formation. The structures that form in the absence of XCTK2 function contain poles that are morphologically normal. In addition, we have assayed the ability of extracts that have been depleted of XCTK2 to form taxol-induced microtubule asters and found that asters form and are indistinguishable from those formed in a control extract (Walczak, C.E., and T.J. Mitchison, unpublished results). If XCTK2 is not important for pole formation in these assays, then what motors are required for pole formation? In *Xenopus* egg extracts, it has been shown that dynein function is required for taxol aster formation (Verde et al., 1991) and for spindle pole formation in a chromatin bead spindle assay (Heald et al., 1996). In both of these assays, the loss of dynein causes a dramatic disruption of the spindle poles or taxol asters, suggesting that dynein provides the major driving force in pole organization in this system. Given the fact that dynein is on the order of 10–50 times more abundant than XCTK2 in these extracts (Verde et al., 1991; Merdes et al., 1996), any pole forming activity that XCTK2 could contribute would be minimal and difficult to assess.

More recent studies in mitotic HeLa cell extracts have demonstrated a complex relationship of motor proteins being involved in spindle pole formation (Gaglio et al., 1996). In these studies, dynein, dynactin, and NuMA (nuclear protein that associates with the mitotic apparatus) all play key roles in the organization of spindle poles. Interestingly, when either dynein or NuMA were depleted in pairs with Eg5 there was a restoration of spindle poles. The authors interpreted these results to suggest the presence of an additional minus end directed motor activity that is associated with NuMA in their extracts, and that spindle pole formation requires a balance of forces produced by different motors. We cannot rule out the possibility that if similar experiments were performed in *Xenopus* spindle assembly assays, we would find similar results. We have analyzed the XCTK2 immunoprecipitates for the presence of NuMA and found no association under the conditions tested, but the association may be more complex and may only occur under conditions of spindle pole formation. In addition, their findings may represent differences between experimental systems where the contribution of different motors varies between systems. Indeed recent studies have shown that NuMA interacts with cytoplasmic dynein in *Xenopus* egg extracts, which suggests that perhaps in frogs, dynein is the most important minus-end motor involved in spindle pole formation (Merdes et al., 1996).

As discussed, the second favored model for COOH-terminal kinesin family members states that these motors provide a counterbalancing force to that of bimC family members. In *Xenopus*, Eg5 is the bimC family member, and it has been shown to be important in spindle pole formation and/or separation (Sawin et al., 1992*a*). In *Xenopus*, when Eg5 and XCTK2 are simultaneously depleted from extracts before spindle assembly, the structures that form look like those of Eg5 depletion alone (Walczak, C.E., and T.J. Mitchison, unpublished observations). Thus

we see no evidence of counterbalancing forces under the conditions tested. One possible explanation for our lack of rescue by loss of both Eg5 and XCTK2 may again be the result of the proportion of force contributed by each of these motors. If in our system dynein is the dominant pole directed force compared to other systems where the XCTK2 motor may make a stronger contribution, then the more interesting combination may be to look at the effect of Eg5 and dynein double depletion on the ability to form spindle poles and spindles.

We propose two models to account for XCTK2 function in *Xenopus.* The first, and perhaps simpler model, proposes that XCTK2 acts to cross-link antiparallel microtubules from two half spindles. As the motor walked to the minus ends of the microtubules at the spindle poles, it would generate a force to draw the two half spindles together into a bipolar spindle. However, there are several reasons why we do not favor this model. First, we would expect a motor that is important in cross-linking of antiparallel microtubules to be enriched in the central spindle. XCTK2 is clearly enriched at the spindle poles and therefore is unlikely to play such a cross-linking role. Second, we would expect that if XCTK2 acted by cross-linking antiparallel microtubules in the central spindle, that antibody addition to preformed spindles would cause those spindles to fall apart. We do not see any effect of antibody addition to preformed spindles. Third, we have looked at the formation of taxol asters in the presence of excess XCTK2 and found significant bundling of microtubules in the asters themselves, but we found no evidence of cross-linking of microtubules from adjacent asters (Walczak, C.E., and T.J. Mitchison, unpublished observations).

We favor a model that implicates XCTK2 in spindle integrity and stability (Fig. 9). In this model, XCTK2 would be important for cross-linking parallel microtubules within each half spindle. A certain level of microtubule bundling and half spindle integrity must be required for the event of half spindle fusion. This model is consistent with our observation that in the absence of XCTK2 function, there is a decrease in the percentage of bipolar spindles that form. We noticed that the bipolar spindles that did form were sometimes less dense or bent, and the half spindles were often splayed. In contrast, addition of excess XCTK2 formed very tightly bundled microtubules within the bipolar spindles that formed. In comparing the results of immunoinhibition of XCTK2 with immunodepletion of XCTK2, we found that the effect of immunodepletion was less severe than immunoinhibition. However, we also found that in a given extract, manipulation of the extract to perform a control immunodepletion caused an approximate twofold reduction in the percentage of bipolar spindles that formed. Under these conditions, there was also an increase in the percentage of half spindles and asters that formed. In these same extracts, immunodepletion of XCTK2 further reduced the percentage of bipolar spindles that formed to levels equivalent to that seen with immunoinhibition in the same extract. These results suggest that any perturbation of the extract that destabilizes half spindle integrity is manifested by a reduction in bipolar spindles that form. We also see a decrease in the percentage of bipolar spindle formation in cycled extracts consistent with the idea that XCTK2 is important for spindle assembly. The inhibition is less dramatic (only a 30% reduction) but significant and provides a good example of how using the two different types of spindle assembly reactions can contribute to our understanding of protein function during spindle assembly.

The idea that a COOH-terminal KRP is involved in spindle stability is not novel. Recent data have shown that spindle assembly in *ncd* mutants is slower than in wild-type cells and that the spindles that do form are unstable and disassemble and then reform with time (Matthies et al., 1996). This live analysis of *ncd* mutants showed that previous groups had seen such a variety of phenotypes in their fixed time point analyses of *ncd* mutant spindles because of the instability of the *ncd* mutant spindles. Our results are quite consistent with the *ncd* data, and we expect that a further comparison of these two proteins may reveal more similarities. It will also be interesting to analyze cytoplasmic dynein mutants during mitosis and meiosis in *Drosophila* and compare it to the *ncd* mutants to understand how different minus end directed motors function in another meiotic system.

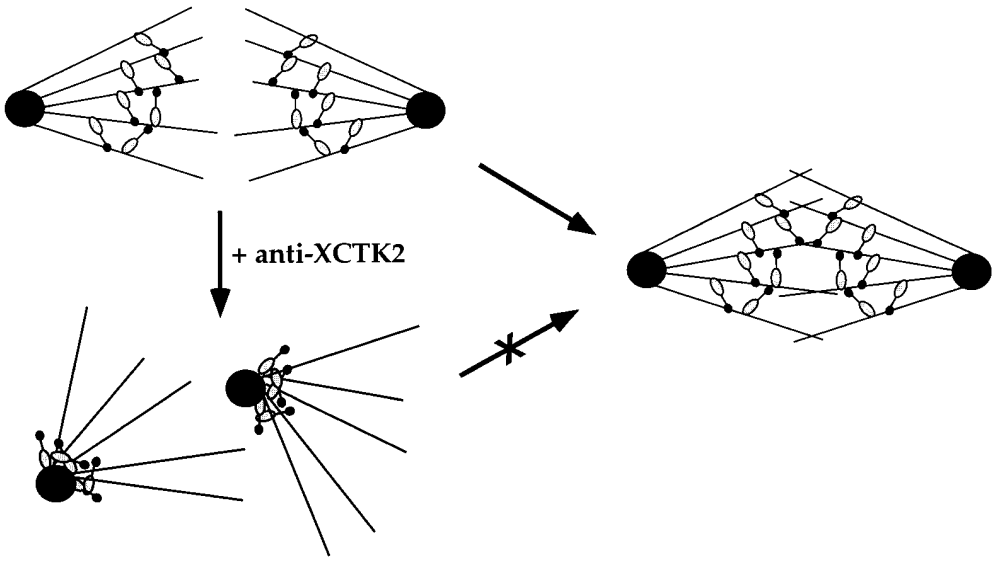

Figure 9. Model for XCTK2 function in spindle assembly. XCTK2 (*lollipops*) is required to bundle microtubules in each half spindle. A certain amount of bundling of microtubules is necessary for efficient fusion of half spindles to occur (*top diagram*). In the presence of anti-XCTK2 antibodies (*lower diagram*), the protein becomes mislocalized toward the spindle poles, and the spindles splay and are incapable of forming bipolar spindles.

XCTK2 Complex Formation and Function In Vivo

Our data indicate that XCTK2 exists in a complex with other proteins in extracts. Furthermore, XCTK2 appears to be a limiting component in this complex. When recombinant XCTK2 was added in excess to extracts, this XCTK2 became incorporated into the complex as evidenced by a shift in S value of the recombinant XCTK2 and by the coimmunoprecipitation of larger amounts of associated proteins.

XCTK2 levels in extracts may be important in controlling the kinetics of spindle assembly. Our data show that XCTK2 is present at ~1–2 μg/ml, a level which is 5–10-fold lower than the amount of other motors in extracts. Even though we tend to think of eggs as a storehouse of proteins required for early divisions of the embryo, the levels of each protein within the egg may need to be precisely regulated. Our earlier studies showed that the level of XKCM1, another *Xenopus* KRP, was important in maintaining proper spindle assembly (Walczak et al., 1996). Likewise, XCTK2 levels also appear to be important. Perhaps XCTK2 function provides a rate-limiting step in the kinetics of spindle assembly. One could imagine that the assembly of a spindle too quickly could lead to detrimental effects and missegregation of chromosomes, an event that would be lethal to the cell. In further support of this idea, our immunofluorescence staining indicates that XCTK2 is sequestered within the nucleus before nuclear envelope breakdown and is taken back up into the reforming daughter nuclei at telophase. It is therefore in the presence of microtubules only during mitosis. We also noticed that the staining of nuclei was abolished sometime after telophase, as evidenced by the lack of staining of nuclei in cells that by morphology had recently divided. This suggests that XCTK2 is degraded and then resynthesized with each cell cycle, another indication that the level of this protein is important. Kuriyama et al. (1995) have made similar observations on the staining pattern of CHO2, the CHO cell homolog of XCTK2. It will be interesting to examine the effects of varying the levels of COOH-terminal KRPs in other systems.

Although kinesin and the heterotrimeric $KRP_{85/95}$ have been shown to associate with nonmotor subunits, no other KRPs have been shown to contain other subunits (for review see Cole and Scholey, 1995). The mitotic KRP, KAR3, has been shown by a two-hybrid analysis and by coimmunoprecipitation experiments to associate with another protein called CIK1 in pheromone-treated cells (Page et al., 1994), suggesting that other COOH-terminal kinesins may also exist in a complex in cells. Much of the analysis of the proteins involved in spindle assembly has focused on the role of motor proteins. However, recent studies have indicated that nonmotor proteins are likely to be of crucial importance in spindle structure and function (Merdes et al., 1996; Echeverri et al., 1996; Gaglio et al., 1995, 1996). The identification and characterization of the other proteins in the XCTK2 complex will be important in understanding how nonmotor proteins function in spindle assembly.

We thank all members of the Mitchison and Alberts labs for helpful comments, criticism, and discussion throughout the course of this work, especially Matt Welch and Karen Oegema for invaluable advice on protein purification and analysis. The Morgan lab provided many helpful suggestions on the use of the baculovirus expression system. We also thank Duane Compton, Rebecca Heald, and Isabelle Vernos for stimulating discussions on motor function in mitosis. Arshad Desai and Matt Welch provided critical comments on this manuscript.

This work was supported by a National Institutes of Health grant and a grant from the Human Frontier Science Program to T.J. Mitchison. C.E. Walczak was supported by a National Institutes of Health post-doctoral fellowship.

Received for publication 30 October 1996 and in revised form 23 December 1996.

References

Ando, A., Y.Y. Kikuti, H. Kawata, N. Okamoto, T. Imai, T. Eki, K. Yokoyama, E. Soeda, T. Ikemura, K. Abe, et al. 1994. Cloning of a new kinesin-related gene located at the centromeric end of the human MHC region. *Immunogenetics.* 39:194–200.

Barton, N.R., and L.S.B. Goldstein. 1996. Going mobile: microtubule motors and chromosome segregation. *Proc. Natl. Acad. Sci. USA.* 93:1735–1742.

Barton, N.R., A.J. Pereira, and L.S.B. Goldstein. 1995. Motor activity and mitotic spindle localization of the *Drosophila* kinesin-like protein KLP61F. *Mol. Biol. Cell.* 6:1563–1574.

Bloom, G., and S. Endow. 1995. Motor proteins 1: kinesins. *Protein Profile.* 2: 1109–1171.

Boleti, H., E. Karsenti, and I. Vernos. 1996. Xklp2, a novel Xenopus centrosomal kinesin-like protein required for centrosome separation during mitosis. *Cell.* 84:49–59.

Chandra, R., E.D. Salmon, H.P. Erickson, A. Lockhart, and S.A. Endow. 1993. Structural and functional domains of the *Drosophila* ncd microtubule motor protein. *J. Biol. Chem.* 268:9005–9013.

Cole, D.G., and J.M. Scholey. 1995. Structural variations among the kinesins. *Trends Cell Biol.* 5:259–262.

Cole, D.G., W.M. Saxton, K.B. Sheehan, and J.M. Scholey. 1994. A slow homotetrameric kinesin-related motor protein purified from *Drosophila* embryos. *J. Biol. Chem.* 269:22913–22916.

Davis, D.G. 1969. Chromosome behavior under the influence of claret-nondisjunctional in *Drosophila melanogaster. Genetics.* 61:577–594.

Echeverri, C.J., B.M. Paschal, K.T. Vaughan, and R.B. Vallee. 1996. Molecular characterization of the 50-kD subunit of dynactin reveals function for the complex in chromosome alignment and spindle organization during mitosis. *J. Cell Biol.* 132:617–633.

Endow, S.A., S.J. Kang, L.L. Satterwhite, M.D. Rose, V.P. Skeen, and E.D. Salmon. 1994. Yeast Kar3 is a minus-end microtubule motor protein that destabilizes microtubules preferentially at the minus ends. *EMBO (Eur. Mol. Biol. Organ.) J.* 13:2708–2713.

Enos, A.P., and N.R. Morris. 1990. Mutation of a gene that encodes a kinesin-like protein blocks nuclear division in *A. nidulans. Cell.* 60:1019–1027.

Eshel, D., L.A. Urrestarazu, S. Vissers, J. Jauniaux, J.C. van Vliet-Reedijk, R.J. Planta, and I.R. Gibbon. 1993. Cytoplasmic dynein is required for normal nuclear segregation in yeast. *Proc. Natl. Acad. Sci. USA.* 90:11172–11176.

Gaglio, T., A. Saredi, and D.A. Compton. 1995. NuMA is required for the organization of microtubules into aster-like mitotic arrays. *J. Cell Biol.* 131:693–708.

Gaglio, T., A. Saredi, J. Bingham, J. Hasbani, S.R. Gill, T.A. Schroer, and D.A. Compton. 1996. Opposing motor activities are required for the organization of the mammalian mitotic spindle pole. *J. Cell Biol.* 135:399–414.

Hagan, I., and M. Yanagida. 1992. Kinesin-related cut7 protein associates with mitotic and meiotic spindles in fission yeast. *Nature (Lond.).* 356:74–76.

Harlow, E., and D. Lane. 1988. Antibodies: A Laboratory Manual. Cold Spring Harbor Laboratory, Cold Spring Harbor, NY.

Hatsumi, M., and S.A. Endow. 1992*a.* The *Drosophila* ncd microtubule motor protein is spindle-associated in meiotic and mitotic cells. *J. Cell Sci.* 103: 1013–1020.

Hatsumi, M., and S.A. Endow. 1992*b.* Mutants of the microtubule motor protein, nonclaret disjunctional, affect spindle structure and chromosome movement in meiosis and mitosis. *J. Cell Sci.* 101:547–559.

Heald, R., R. Tournebize, T. Blank, R. Sandaltzopoulos, P. Becker, A. Hyman, and W. Karsenti. 1996. Self-organization of microtubules into bipolar spindles around artificial chromosomes in *Xenopus* egg extracts. *Nature* (*Lond.*). 382:420–425.

Hirano, T., and T.J. Mitchison. 1993. Topoisomerase II does not play a scaffolding role in the organization of mitotic chromosomes assembled in *Xenopus* egg extracts. *J. Cell Biol.* 120:601–612.

Hoyt, M.A., L. He, K.K. Loo, and W.S. Saunders. 1992. Two *Saccharomyces cerevisiae* kinesin-related gene products required for mitotic spindle assembly. *J. Cell Biol.* 118:109–120.

Hoyt, M.A., L. He, L. Totis, and W.S. Saunders. 1993. Loss of function of *Saccharomyces cerevisiae* kinesin-related *CIN8* and *KIP1* is suppressed by *KAR3* motor domain mutations. *Genetics.* 135:35–44.

Kashina, A.S., J.M. Scholey, J.D. Leszyk, and W.M. Saxton. 1996. An essential bipolar mitotic motor. *Nature (Lond.).* 384:225.

Kuriyama, R., M. Kofron, R. Essner, T. Kato, S. Dragas-Granoic, C.K. Omoto,

and A. Khodjakov. 1995. Characterization of a minus end-directed kinesin-like motor protein from cultured mammalian cells. *J. Cell Biol.* 129:1049–1059.

Li, Y., E. Yeh, T. Hays, and K. Bloom. 1993. Disruption of mitotic spindle orientation in a yeast dynein mutant. *Proc. Natl. Acad. Sci. USA*. 90:10096–10100.

Lohka, M.J., and J.L. Maller. 1985. Induction of nuclear envelope breakdown, chromosome condensation, and spindle formation in cell-free extracts. *J. Cell Biol.* 101:518–523.

Matthies, H.J.G., H.B. McDonald, L.S.B. Goldstein, and W.E. Theurkauf. 1996. Anastral meiotic spindle morphogenesis: role of the nonclaret disjunctional kinesin-like protein. *J. Cell Biol.* 134:455–464.

McDonald, H.B., R.J. Stewart, and L.S.B. Goldstein. 1990. The kinesin like ncd protein is a minus end directed microtubule motor. *Cell.* 63:1159–1165.

Meluh, P.B., and M.D. Rose. 1990. KAR3, a kinesin-related gene required for yeast nuclear fusion. *Cell.* 60:1029–1041.

Merdes, A., K. Ramyar, J.D. Vechio, and D.W. Cleveland. 1996. A complex of NuMA and cytoplasmic dynein is essential for mitotic spindle assembly. *Cell.* 87:447–458.

Moore, J.D., and S.A. Endow. 1995. Kinesin proteins: a phylum of motors for microtubule-based motility. *Bioessays.* 18:207–219.

Murray, A.W. 1991. Cell cycle extracts. *In* Methods in Cell Biology. Vol. 36. B.K. Kay and H.B. Peng, editors. Academic Press Inc., San Diego, CA. pp. 581–605.

O'Connell, M.J., P.B. Meluh, M.D. Rose, and N.R. Morris. 1993. Suppression of the bimC4 mitotic spindle defect by deletion of klpA, a gene encoding a kar3-related kinesin-like protein in *Aspergillus nidulans. J. Cell Biol.* 120: 153–162.

Page, B.D., L.L. Satterwhite, M.D. Rose, and M. Snyder. 1994. Localization of the Kar3 kinesin heavy chain-related protein requires the Cik1 interacting protein. *J. Cell Biol.* 124:507–519.

Pfarr, C.M., M. Coue, P.M. Grisson, T.S. Hays, M.E. Porter, and J.R. McIntosh. 1990. Cytoplasmic dynein is localized to kinetochores during mitosis. *Nature (Lond.)*. 345:263–265.

Pidoux, A.L., M. LeDizet, and W.Z. Cande. 1996. Fission yeast pkl1 is a kinesin-related protein involved in mitotic spindle function. *Mol. Biol. Cell.* 7: 1639–1655.

Roof, D.M., P.B. Meluh, and M.D. Rose. 1992. Kinesin-related proteins required for assembly of the mitotic spindle. *J. Cell Biol.* 118:95–108.

Saunders, W.S., and M.A. Hoyt. 1992. Kinesin-related proteins required for structural integrity of the mitotic spindle. *Cell.* 70:451–458.

Saunders, W.S., D. Koshland, D. Eshel, I.R. Gibbons, and M.A. Hoyt. 1995. *Saccharomyces cerevisiae* kinesin- and dynein-related proteins required for anaphase chromosome segration. *J. Cell Biol.* 128:617–624.

Sawin, K.E., and T.J. Mitchison. 1991. Mitotic spindle assembly by two different pathways in vitro. *J. Cell Biol.* 112:925–940.

Sawin, K.E., and S.A. Endow. 1993. Meiosis, mitosis and microtubule motors. *Bioessays.* 15:399–407.

Sawin, K.E., K. LeGuellec, M. Philippe, and T.J. Mitchison. 1992*a.* Mitotic spindle organization by a plus-end directed microtubule motor. *Nature (Lond.).* 359:540–543.

Sawin, K.E., T.J. Mitchison, and L.G. Wordeman. 1992*b*. Evidence for kinesin-like proteins in the mitotic apparatus using peptide antibodies. *J. Cell Sci.* 102:303–313.

Shamu, C.E., and A.W. Murray. 1992. Sister chromatid separation in frog egg extracts requires DNA topoisomerase II activity during anaphase. *J. Cell Biol.* 117:921–934.

Siegel, L.W., and K.J. Monty. 1966. Determination of molecular weights and frictional ratios of proteins in impure systems by use of gel filtration and density gradient centrifugation. Application to crude preparations of sulfite and hydroxylamine reductases. *Biochim. Biophys. Acta.* 112:346–362.

Smith, D.B., M.R. Rubira, R.J. Simpson, K.M. Davern, W.U. Tui, P.G. Board, and G.F. Mitchell. 1988. Expression of an enzymatically-active parasite molecule in *Escherichia coli*: *Schistosoma japonicum* glutathione S-transferase. *Mol. Biochem. Parasitol.* 27:249–256.

Steuer, E.R., L. Wordeman, T.A. Schroer, and M.P. Sheetz. 1990. Localization of cytoplasmic dynein to mitotic spindles and kinetochores. *Nature (Lond.).* 345:266–268.

Vaisberg, E.A., M.P. Koonce, and J.R. McIntosh. 1993. Cytoplasmic dynein plays a role in mammalian mitotic spindle formation. *J. Cell Biol.* 123:849–858.

Verde, F., J.-M. Berrez, C. Antony, and E. Karsenti. 1991. Taxol-induced microtubule asters in mitotic extracts of *Xenopus* eggs: requirement for phosphorylated factors and cytoplasmic dynein. *J. Cell Biol.* 112:1177–1188.

Vernos, I., and E. Karsenti. 1996. Motors involved in spindle assembly and chromosome segregation. *Curr. Opin. Cell Biol.* 8:4–9.

Vernos, I., J. Raats, T. Hirano, J. Heasman, E. Karsenti, and C. Wylie. 1995. Xklp1, a chromosomal *Xenopus* kinesin-like protein essential for spindle organization and chromosome positioning. *Cell.* 81:117–127.

Walczak, C.E., T.J. Mitchison, and A. Desai. 1996. XKCM1: A *Xenopus* kinesin-related protein that regulates microtubule dynamics during mitotic spindle assembly. *Cell.* 84:37–47.

Walker, R.A., E.D. Salmon, and S.A. Endow. 1990. The *Drosophila* claret segregation protein is a minus-end directed motor molecule. *Nature (Lond.).* 347:780–782.